Evaluation of explosion characteristics of 2-methylfuran/air mixture

Oppong, F., Xu, C., Zhongyang, L., Li, X., Zhou, W. & Wang, C.

Original citation & hyperlink:
Oppong, F, Xu, C, Zhongyang, L, Li, X, Zhou, W & Wang, C 2019, 'Evaluation of explosion characteristics of 2-methylfuran/air mixture', Journal of Loss Prevention in the Process Industries, vol. 62, 103954.
https://dx.doi.org/10.1016/j.jlp.2019.103954

DOI 10.1016/j.jlp.2019.103954
ISSN 0950-4230

Publisher: Elsevier

Journal Pre-proof

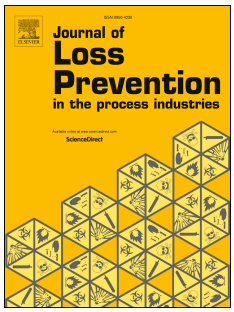

Evaluation of explosion characteristics of 2-methylfuran/air mixture

Francis Oppong, Cangsu Xu, Luo Zhongyang, Xiaolu Li, Wenhua Zhou, Chongming Wang

PII: S0950-4230(19)30543-1

DOI: https://doi.org/10.1016/j.jlp.2019.103954

Reference: JLPP 103954

To appear in: *Journal of Loss Prevention in the Process Industries*

Received Date: 1 July 2019

Revised Date: 5 September 2019

Accepted Date: 5 September 2019

Please cite this article as: Oppong, F., Xu, C., Zhongyang, L., Li, X., Zhou, W., Wang, C., Evaluation of explosion characteristics of 2-methylfuran/air mixture, *Journal of Loss Prevention in the Process Industries* (2019), doi: https://doi.org/10.1016/j.jlp.2019.103954.

Evaluation of explosion characteristics of 2-methylfuran/air mixture

Francis Oppong[a], Cangsu Xu[a*], Luo Zhongyang[a], Xiaolu Li[b], Wenhua Zhou[a], Chongming Wang[c]

[a]*College of Energy Engineering, State Key Laboratory of Clean Energy Utilization, Zhejiang University, Hangzhou, 310027, China P.R.*

[b]*College of Mechanical and Electrical Engineering, China Jiliang University, Hangzhou, 310018, China P.R.*

[c] *School of Mechanical, Aerospace and Automotive Engineering, Coventry University, Coventry, CV1 5FB, United Kingdom.*

**Corresponding author: xucangsu@zju.edu.cn, Tel: +86 135 0581 4628*

Evaluation of explosion characteristics of 2-methylfuran/air mixture

Abstract

Herein, the explosion characteristics such as the peak explosion pressure, maximum pressure rise rate and deflagration index of 2-methylfuran (MF) /air mixture have been investigated at high pressures and temperatures. Knowledge of these parameters can be used in the safety assessment of MF explosions. The explosion experiments were performed at the initial pressure of 1, 2, 3, and 4 bar, the initial temperature of 333, 363, 393, and 423 K and the equivalence ratio of 0.7-1.4 using a constant volume combustion bomb. The pressure data obtained from the experiment were carefully processed to examine MF peak explosion pressure, maximum pressure rise rate, explosion time as well as the deflagration index. Explosion characteristics of MF were sensitive to the initial pressure and temperature conditions and the mixture concentration. An increment in the initial pressure triggered a dramatic growth in the peak explosion pressure, maximum rate of pressure rise and the deflagration index. Alternatively, an increment in the initial temperature decreased the peak explosion pressure, maximum pressure rise rate and the deflagration index. By and large, MF explosion parameters obtained in this investigation can offer firsthand information on MF explosion hazard assessment at high pressures and temperatures.

Keywords: 2-methylfuran (MF); Explosion characteristics; Explosion pressure; Pressure rise rate; Deflagration index; Explosion time

Nomenclature

V	Combustion vessel volume, m^3
T	Temperature, K
p	Explosion pressure, bar
p_{max}	Peak explosion pressure, bar
dp/d_{max}	Maximum pressure rise rate, bar/s
	Time after ignition, ms
	Explosion time, ms
$_e$	End of explosion time, ms
dp/d	Pressure rise rate, bar/s
T_i	Initial temperature, K
p_i	Initial pressure, bar
S_L	Laminar burning velocity, m/s
K_G	Deflagration index, bar*m/s

Subscript

max	Maximum
i	Initial
L	Laminar
c	Combustion
e	End

Greek Symbol

ϕ	Equivalence ratio

1. Introduction

Annually, chemical or gas explosion accident kill and injure hundreds of people globally (Beck, 2016; OECD, 2013; World Health Organization, 2009; Wu et al., 2019). As a matter of fact, an explosion can occur in industries, household, confined and unconfined space, process equipment as well as in offshore/marine structures when a flammable gas or highly evaporative liquid is accidentally discharged into the atmosphere and meet a strong ignition source. In compliance with this, the explosion characteristics of distinct flammable or highly evaporative fuels have to be thoroughly studied. To this end, having knowledge of the explosion characteristics such as the peak explosion pressure, maximum pressure rise rate, explosion time and deflagration index is useful to improve safety. In essence, the deflagration index is used as the foundation for the design of pressure tanks and safety relief valves for chemical storage as well as vents, high pressure and temperature combustors/furnace. The magnitude of the deflagration index characteristically determines the severity of the explosion. Therefore, higher deflagration indices/values indicate the possibility of extremely dangerous explosion. Considerable investigations have been performed in the literature to study the explosive behavior of gaseous and liquid fuels in recent years. Just to mention a few, quite a bit of these investigations used hydrogen (Li et al., 2015; Li et al., 2018a, 2018b; Sun and Li, 2017), methane/methanol (Cui et al., 2018; Kundu et al., 2018; Mitu and Brandes, 2015; Tang et al., 2014), ethanol (Mitu et al., 2018; Mitu and Brandes, 2017) and syngas (Tran et al., 2017) fuels. The authors sought to investigate the impact of initial pressure, initial temperature and equivalence ratio on the peak explosion pressure, maximum rate of pressure rise, explosion time and deflagration index of these fuels. For instance, Hu et al. (2017) have investigated the explosion characteristics of butanol/isooctane blends and corroborated that at rich mixtures and elevated pressures the peak pressure exhibited oscillatory behaviour which reduced the explosion time and increased the maximum pressure rise rate. In another study, Shen et al. (2017b) showed that methane has a higher upper flammability limit than ethane. What's more, Li et al. (2015) have evaluated the explosion characteristics of alcohol (ethanol, 1-butanol, 1-pentanol) /air mixtures. Their results showed that 1-pentanol had the largest peak explosion pressure and maximum pressure rise rate on the rich regime of the mixture when compared with ethanol and 1-butanol. They asserted that this occurrence was due to the difference in heat loss of the various alcohols. On one hand, the maximum pressure rise rate was insensitive to the initial temperature variation. More recently, Sun (2018) also studied the explosion properties of syngas and reported that within his investigated conditions the deflagration index was below 30 MPa*m/s.

Laminar burning velocity (LBV) is another significant parameter which quantifies the physicochemical properties of premixed flames/combustion. Essentially, it is used to validate the chemical mechanism of a specific fuel and gives essential information about the burning process and flame dynamics (Bao et al., 2017). The burning velocity of a premixture is somehow related to the explosion pressure development, meanwhile, it is very influential in predicting explosion hazards (Huzayyin et al., 2008). Several studies have been performed to study the burning speeds of different fuels in the literature (Askari et al., 2017; Mannaa et al., 2015; Mitu et al., 2015; Reyes et al., 2018). Moreover, some of these studies evaluated the correlation between the burning velocity and explosion parameters (Dahoe, 2005; Dahoe and de Goey, 2003; Saeed, 2017; Zhang et al., 2019b). Recently, Ma et al., (2013a, 2013b) studied the burning characteristics of 2-methylfuran (MF) / air mixtures and reported that MF had unstable flames and higher burning velocities

compared to isooctane and 2,5-dimethylfuran. In another study, the following researchers (Somers et al., 2013; Xu et al., 2018; Zhongyang et al., 2018) also studied the LBV of 2-methylfuran at elevated pressures and temperatures and evaluated the correlation between the burning velocities and the initial pressure and temperature.

In the meantime, in the long haul, 2-methylfuran has the potential as an alternative fuel. In addition, it also used in the pharmaceutical industry and the manufacturing of pesticides. MF is highly flammable, has a lower flash point and easy to vaporize, therefore, any leakage of MF poses a potential threat to human life and properties. If MF is inappropriately handled during production, transportation and storage it can cause a fire outbreak as well as an explosion if any leaked MF meets a strong ignition source. Therefore, firsthand information about its explosion characteristics is relevant for accident and safety evaluations. In spite of the progress made in the investigation of explosion characteristics of many fuels in previous publications, to the best knowledge of the authors, there is no information on MF explosion characteristics such as the peak explosion pressure, maximum pressure rise rate, explosion time and deflagration index in the literature. In addition, the explosion characteristics of liquid fuels, most especially liquid biofuels are rarely studied in the literature. Therefore, this work intends to examine the explosion features of 2-methylfuran at elevated pressures and temperatures. The main purpose of this work is to investigate the influence of initial pressure, initial temperature and the equivalence ratio on MF explosion. 2-methylfuran explosion characteristics were experimentally determined using a constant volume combustion chamber (CVCC) at the initial temperature (333, 363, 393 and 423 K), initial pressure (1, 2, 3, and 4 bar) and equivalence ratio (0.7-1.4). The experimental explosion pressure data were well examined to determine MF peak explosion pressure, maximum pressure rise rate and explosion time. Last but most definitely not least, 2-methylfuran LBV data were mapped against the equivalence ratio.

2. Analysis of experimental device and method

The experimental instrumentation has been shown elsewhere (Zhongyang et al., 2018). The experiment was done in a CVCC which has an inner length to diameter ratio of (L/D = 1.0). The CVCC has an inner volume of 2.067 L. In addition, experimental data of the testing rig have been validated in this paper (Zhongyang et al., 2018). The CVCC also comprises of a high-speed imaging (Schlieren) system and a data recording system. It also has quartz windows which permits viewing and recording of flame images. The CVCC has six heating units on its sides used to control the initial temperature. Moreover, the initial mixture temperature was measured with a K-Type thermocouple (WRNK-231) which is accurate to ±0.75%. Altogether the combustion pressure was recorded by a piezoelectric pressure sensor (Kistler 6115A) and a charge amplifier (Kistler 5018A). Meanwhile, the initial pressure was determined with a high precision pressure gauge (Keller LEX1). The resolution of the pressure sensor is 0.0001 MPa. Therefore, 0.1-3% of inaccuracy was generated by the initial pressure. The sampling frequency of the pressure recording unit is 75MHz. The mixture was ignited with two electrodes of diameter 0.4mm opposite with each other and the ignition unit. The ignition or spark energy of the experiment is 10mJ (Xu et al., 2014). The mean of three testing data was used for each ϕ in order to warrant 90-95% certitude.

3. Results and discussion

The experimentally recorded pressure data have some level of noise in the data; therefore, it is difficult and inaccurate to determine the explosion parameters from the raw pressure data. In this regard, the raw pressure history was filtered or smoothed using a low-pass band filter in Python. Fig. 1 shows a typical example of smooth explosion pressure (p) and pressure rise rate (dp/d) cartography at the initial pressure (p_i) of 2 bar, the initial temperature (T_i) of 393 K and stoichiometric fuel/air ratio of ϕ = 1.0. As shown in Fig. 1, the pressure steadily increases after ignition and reaches the peak at p_{max}. However, after obtaining p_{max} the pressure starts to drop due to heat loss to the CVCC wall when the flame front reaches the wall. The combustion/explosion time was attained at the time ( ). The maximum pressure rise rate was recorded at the point (dp/d $_{max}$). At last, the combustion process was completed at the time ($_e$). It is worth to mention that p_{max}, , and dp/d $_{max}$ are the important parameters typically used in the safety assessment of a specific fuel/chemical, hence, herein they are the only parameters discussed.

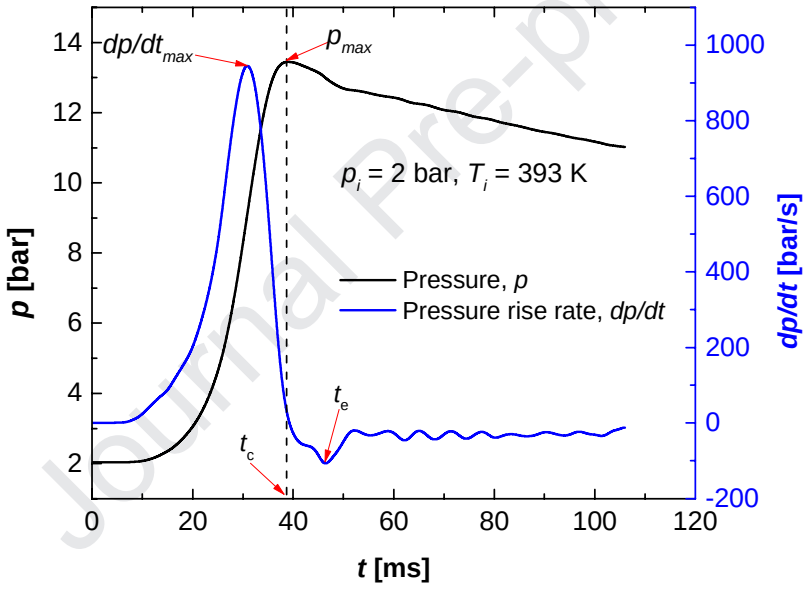

Fig. 1. Illustration of in-chamber explosion pressure evolution and pressure rise rate contours at T_i = 393 K and p_i = 2 bar and ϕ = 1.0.

3.1. Explosion pressure and peak explosion pressure

Fig. 2 shows p contours at p_i = 4 bar and T_i = 423 K for different ϕ. Similar contours were obtained for the different p_i, T_i and ϕ values investigated in this document. With reference to Fig. 2, it can be noticed that the value of p is sensitive to ϕ, therefore, the magnitude of p increases with increasing ϕ. Parallel trends have been observed in previous studies (Li et al., 2015, Cui et al., 2018; Mitu and Brandes, 2015; Tang et al., 2014). The reduced amount of fuel at ϕ = 0.7 and 0.9 led to less heat energy released from the combustion phenomena and lower p values. The opposite is true for ϕ = 1.0, 1.1 and 1.2. The peak value of p increased from 20.593 bar to 26.495 bar when ϕ increased from 0.7 to 1.2. Fig. 3 displays p values at p_i = 4 bar, T_i = 363-423 K and ϕ = 1.0. The magnitude

of p is lower at a higher T_i owing to a higher mass burning rate and flame speed at a higher T_i. Accordingly, the combustible mixture takes a shorter time to reach the peak of p. In addition to this, the mass of MF/air unburnt mixture in the CVCC was decreased (less heat energy from combustion) at a higher T_i, thence, leading to the decreased peak value of p. The peak values of p obtained at 363 K, 393 K and 423 K are 29.577 bar, 27.084 bar, and 25.364 bar. Furthermore, it can be noticed in Fig. 4 that an increment in the value of p_i increased the magnitude of p due to the robustness of the combustion process which generated a higher amount of heat energy. The highest values of p increased from 6.077 bar to 25.364 bar when the value of p_i increased from 1 bar to 4 bar.

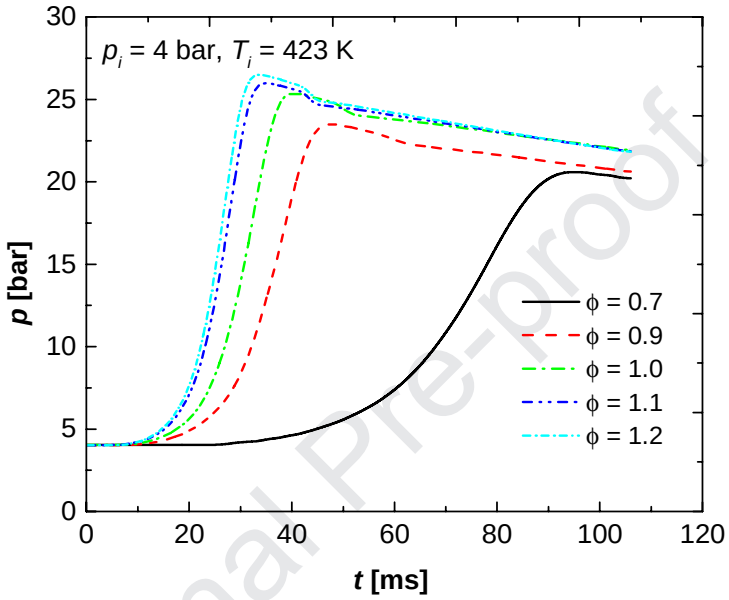

Fig. 2. In-chamber p evolution versus at ϕ = 0.7-1.2, T_i = 423 K and p_i = 4 bar.

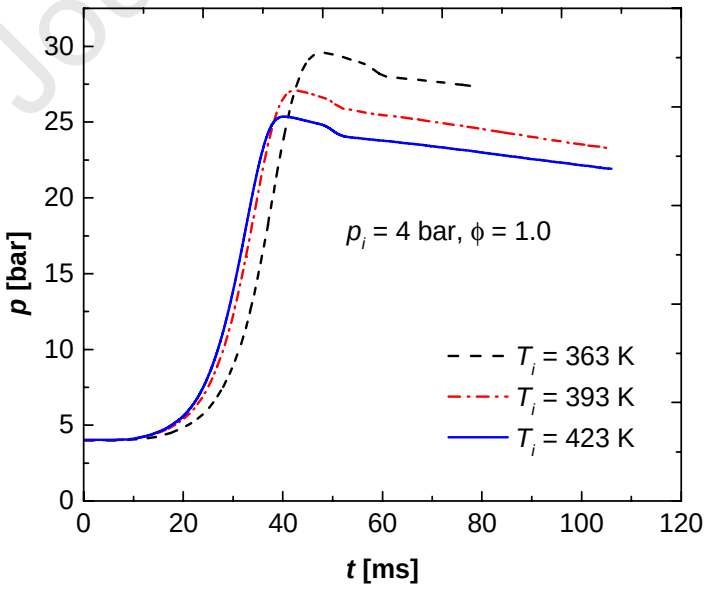

Fig. 3. A plot of p versus at T_i = 363-423 K, p_i = 4 bar and ϕ = 1.0.

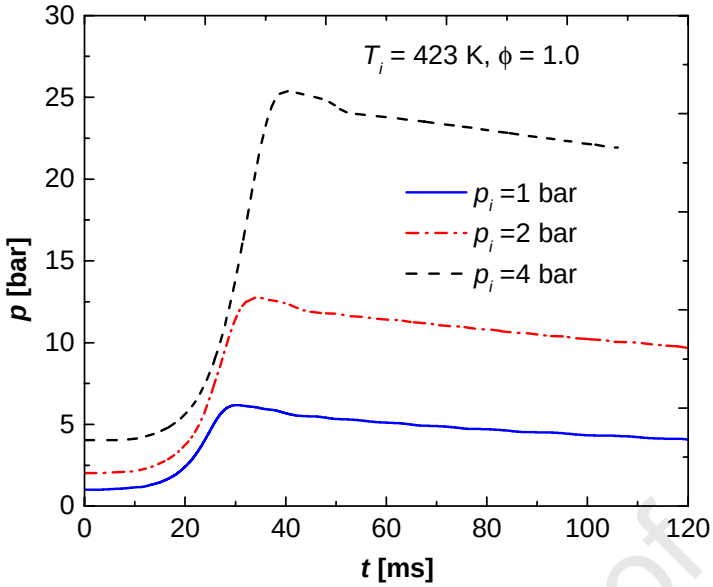

Fig. 4. A plot of p against at T_i = 423 K, p_i = 1-4 bar and ϕ = 1.0.

The peak explosion pressure (p_{max}) quantify the energy distribution of combustion propagating waves (Shen et al., 2017b). Therefore, p_{max} can be used to determine the heat energy from the explosion. Fig. 5 depicts the values of p_{max} as a function of ϕ at p_i = 1-4 bar and T_i= 363-423 K. In general, the values of p_{max} increases with increasing ϕ. In lean mixtures, the amount of MF fuel in the CVCC is less leading to less release of heat energy and lower p_{max}. On the other hand, combustion becomes more robust as ϕ increases, consequently, the value of p_{max} also increases. As shown in Fig. 5, somewhat p_{max} decreases at some of the rich mixtures due to an insufficient amount of oxygen in the CVCC leading to incomplete combustion and a reduced amount of heat released.

Furthermore, the values of p_{max} are somehow higher at a lower T_i and increases dramatically as p_i increases. The reason for a higher p_{max} at a lower T_i is due to the increased mass of the unburnt MF mixture in the CVCC (higher heat energy from MF explosion) which subsequently increased the value of p_{max}. Again, a total reduction in the burning mass of MF mixture and heat loss could also possibly cause a decrease in the explosion peak pressure when T_i was increased. On one hand, at a higher p_i MF explosion becomes more and more energetic leading to a higher release of thermal energy, and a higher p_{max} as depicted in Fig. 5.

The experimental p_{max} data are compared to simulated p_{max} data in Fig. 6. The numerical data were obtained using constant-volume combustion in CANTERA (Goodwin et al., 2017) and MF comprehensive chemical mechanism (Cheng et al., 2017). Comparatively, the experimental p_{max} values are lower than the simulated results. The disparity between the experiment and the simulated p_{max} is attributable to heat loss (conduction and radiation) in the CVCC during the experiment which reduces the pressure rise whereas the numerical analysis assumes adiabatic condition. In addition, somehow some of the fuel could be stuck in the vessel due to adsorption and couldn't burn during combustion, which could lead to reduced peak pressures (Zhang et al., 2019a). Moreover, likewise, the observations made in Fig. 5, an increment in the initial pressure promotes strenuous combustion and the release of higher thermal energy and peak explosion pressures.

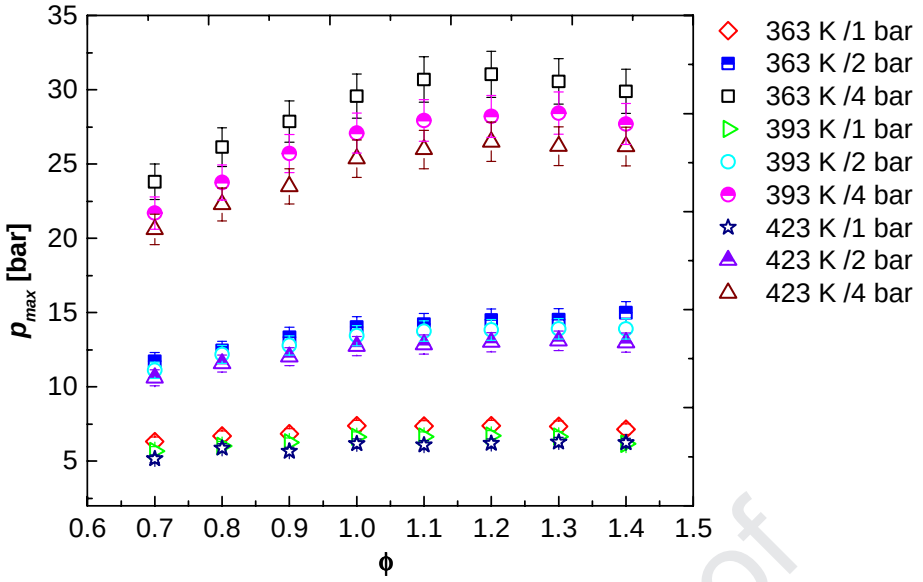

Fig. 5. A chart of p_{max} against ϕ at T_i = 363-423 K and p_i = 1-4 bar. Legend: p_i is led by T_i.

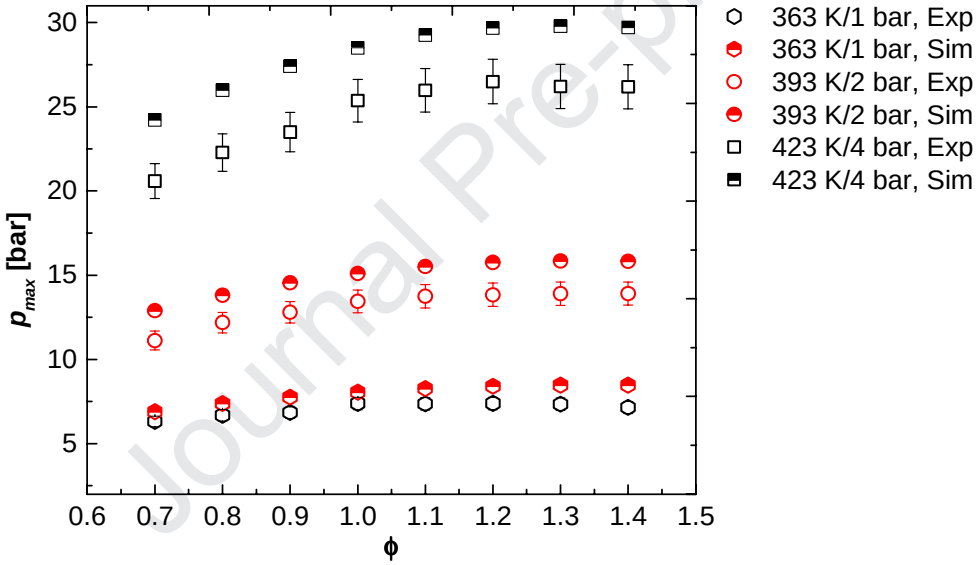

Fig. 6. Experimental and simulated p_{max} at T_i = 363, 393, and 423 K, p_i = 1, 2, and 4 bar and ϕ = 0.7-1.4. Legend: p_i is led by T_i. Exp and Sim refer to the experimental and simulated results.

Fig. 7 describes the effect of p_i on p_{max} at ϕ = 0.8, 1.0, and 1.2 and T_i of 363 K. In conformity with Fig. 7, it can be realized that in someway p_i increases linearly with p_{max}values. The explosion becomes brisk when p_i is increased which will lead to a higher discharge of heat from the combustion and high pressure rise. Here, as the values of p_i increased from 1 bar to 4 bar, p_{max} values also increased from 6.689-26.139 bar (ϕ = 0.8), 7.388-29.577 bar (ϕ = 1.0) and 7.388-31.041 bar at ϕ = 1.2. Fig. 8 also illustrates the impact of T_i on p_{max} at p_i of 4 bar and ϕ = 0.8, 1.0, and 1.2. Similar correlations have been noticed in past studies (Mitu et al., 2012; Saeed, 2017) for distinct fuels. As can be observed in Fig. 8, p_{max} values somehow decrease linearly with increasing T_i. When T_i was increased the density of MF mixture in the CVCC decreased which resulted in rapid burning speed and decreased p_{max} values. When T_i increased from 333 K to 423 K, p_{max}

decreased from 28.057 bar to 22.285 bar at (ϕ = 0.8). At the same time, p_{max} decreased from 31.553 bar to 25.364 bar at (ϕ = 1.0) as well as 31.677 bar to 26.495 bar at (ϕ = 1.2) when T_i increased from 333 K to 423 K.

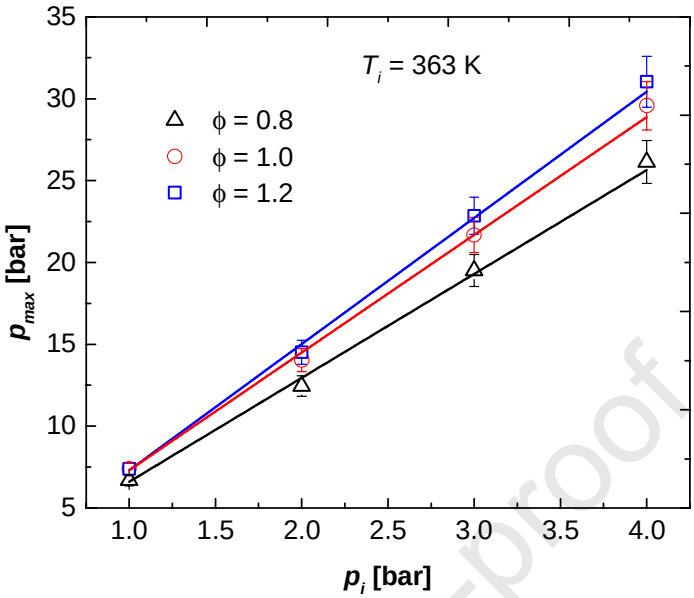

Fig. 7. Effect of p_i on p_{max} at ϕ = 0.8, 1.0, and 1.2 and T_i = 363 K. The solid lines are linear fit.

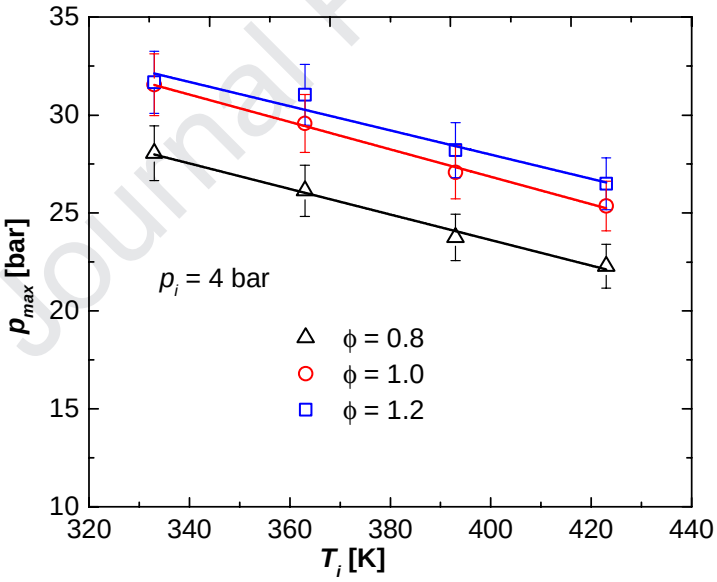

Fig. 8. Effect of T_i on p_{max} at ϕ = 0.8, 1.0, and 1.2 and p_i = 4 bar. The solid lines are linear fit.

3.2. Pressure rise rate, maximum pressure rise rate and deflagration index

Fig. 9 displays the plot of pressure rise rate (dp/d) versus at ϕ = 0.7-1.2, p_i = 4 bar and T_i = 423 K. As can be observed in Fig. 9, for each of the dp/d map (ϕ = 0.7-1.2), dp/d initially increases and reaches the maximum value and decrease afterwards. Moreover, due to excessive heat transfer to the CVCC wall the explosion pressure p decreases and the values of dp/d become

negative as illustrated in Fig.9. In accordance with Fig. 9, the values of dp/d somehow increases with increasing ϕ, underlining the sensitivity of dp/d to ϕ. The peak of dp/d value increased from 571.3 bar/s to 2147.3 bar/s when ϕ increased from ϕ = 0.7 to 1.2, obtaining the highest value at ϕ = 1.2. Fig. 10 also shows the comparison of dp/d at T_i = 363, 393 and 423 K, p_i = 1 bar and ϕ = 1.0.

According to Fig. 10, the peak of dp/d increases with a lower T_i. Thus, increased MF burning velocity or speed as well as decreased explosion pressure and maximum pressure rise rate depends on increased T_i. The highest values of dp/d are 542.905 bar/s (363 K), 509.712 bar/s (393 K) and 444.523 bar/s for 423 K. Fig. 11 represents the variation of dp/d with p_i at T_i = 423 K and ϕ = 1.0. As shown in Fig. 11, the values of dp/d almost increased twofold with increased p_i. In addition, when p_i increased from 1 bar to 4 bar the value of dp/d increased from 444.523 bar/s to 1668.99 bar/s. As aforementioned in Section 3.1, this could be due to more and more energetic MF explosion at increased p_i.

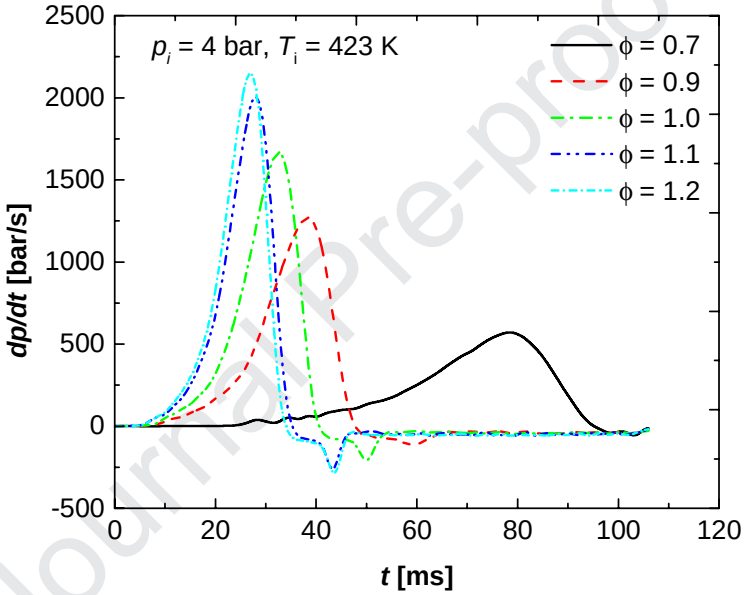

Fig. 9. A graph of pressure rise rate contours at T_i = 423 K, p_i = 4 bar and ϕ = 0.7-1.2.

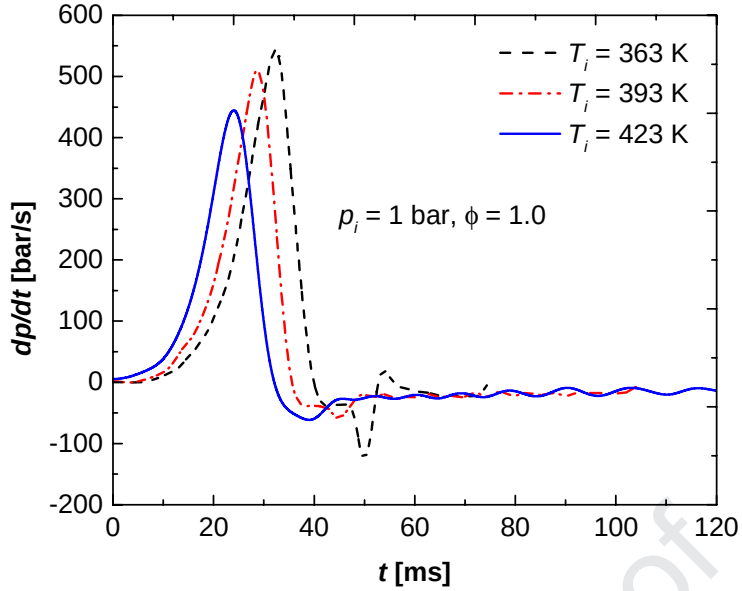

Fig. 10. Pressure rise rate maps at p_i = 1 bar, T_i = 363-423 K and ϕ = 1.0.

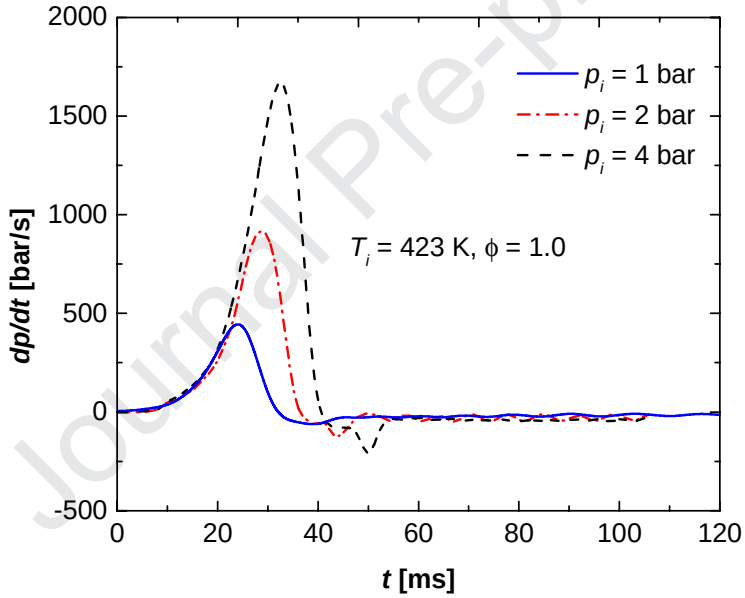

Fig. 11. Effects of p_i on dp/d at T_i = 423 K and ϕ = 1.0.

The maximum pressure rise rate $dp/d\ _{max}$ is a significant parameter used to describe the explosion build-up pressure. It is a very influential parameter in the estimation of the deflagration index (K_G). Fig. 12 compares $dp/d\ _{max}$ at T_i = 363-423 K, p_i = 1-4 bar and ϕ = 0.7-1.4. As depicted in Fig. 12, $dp/d\ _{max}$ values are fairly higher at a lower T_i when compared to $dp/d\ _{max}$ values at a higher T_i. Truly, increased T_i dictates higher burning velocity and reduced p_{max}. However, the combined effect of the burning velocity and p_{max} determines the magnitude of the maximum pressure rise rate. In addition, the values of $dp/d\ _{max}$ increases drastically when p_i increases. As shown in Fig. 12, $dp/d\ _{max}$ values are somehow insensitive to p_i at some of the equivalence ratios.

The deflagration index (K_G) measures the intensity of the combustion or explosion process. Therefore, the higher the value of the deflagration index the more intense the explosion risk. The deflagration index forms the basis for the design of explosion devices and safety assessment. Fundamentally, the deflagration index is quantified as, $K_G = dp/d_{max}.V^{1/3}$ (Dahoe and de Goey, 2003; Saeed, 2017). V denotes the CVCC inner volume. Invariably, explosion advancement is influenced by the volume of a vessel. Accordingly, an increment in the volume (radius) of a vessel results in an increment in the flame propagation time. Therefore, the pressure rise during the explosion is volume-variant. However, according to the definition of cube-root law or K_G, multiplying dp/d_{max} by $V^{1/3}$ renders K_G volume-independent irrespective of the vessel size (Dahoe, 2005; Dahoe and de Goey, 2003; Faghih et al., 2016; Xie et al., 2016). Thus, dp/d_{max} is normalized by $V^{1/3}$.

Again, Fig. 12 shows K_G values graphed against ϕ at T_i = 363-423 K and p_i = 1-4 bar. The values of K_G have a similar tendency as dp/d_{max}due to its linear dependence on dp/d_{max}. The magnitude of K_G values rise with increased ϕ. Besides, an increment in p_i dramatically increases K_G values due to more vigorous combustion. Thus, at a higher p_i, the propagating flame front becomes more vigorous and instable, hence, generating a higher p_{max} and dp/d_{max} as well as K_G. Herein, K_G values of MF range from 200-300 bar*m/s at p_i = 4 bar, T_i = 363 K, 393 K and 423 K, and ϕ = 1.0-1.4. Fig. 13 also depicts the variation of dp/d_{max} with p_i at T_i = 393 K and ϕ = 0.8, 1.0, and 1.2. Fig. 13 discloses that MF dp/d_{max} values are greater at a higher p_i and to a certain degree varies linearly with p_i values. Herein, dp/d_{max} increased from 315.645-886.725 bar/s (ϕ = 0.8), 509.712-1728.69 bar/s (ϕ = 1.0), and 545.877-2192.92 bar/s (ϕ = 1.2) when p_i increased from 1 bar to 4 bar.

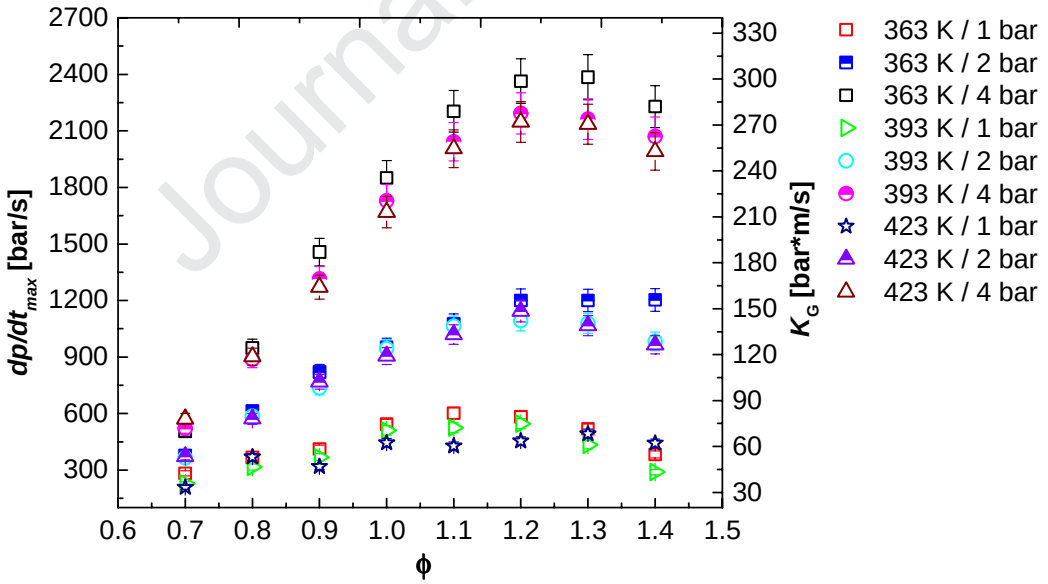

Fig. 12. dp/d_{max} and K_G plots with ϕ at p_i = 1-4 bar and T_i = 363-423 K. Legend: p_i is led by T_i.

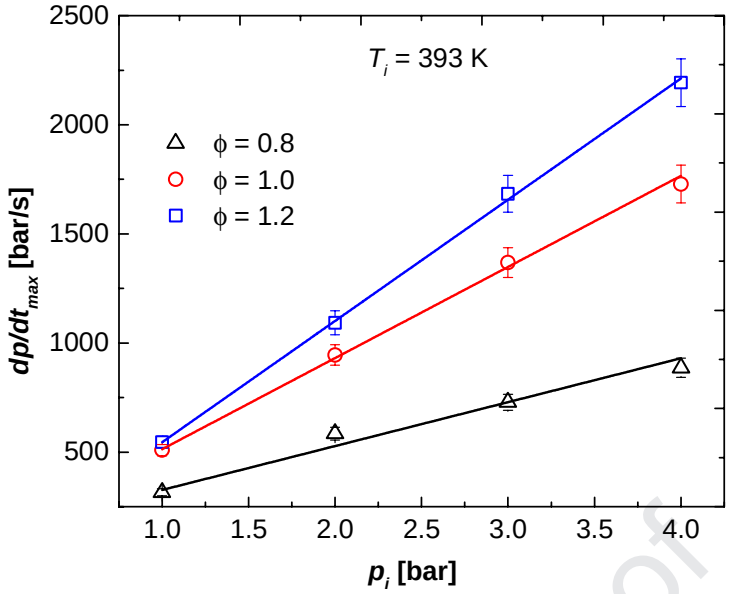

Fig. 13. A chart of $dp/d\ _{max}$ against p_i at T_i = 393 K and ϕ = 0.8, 1.0, and 1.2. The solid lines are linear fit.

3.3. Explosion time

Herein, the explosion time ( ) describes the time at which p_{max} was obtained. The explosion time is very crucial in safety assessment and design of combustion devices. Fig. 14 shows values at the investigated conditions, p_i = 2 and 4 bar and T_i = 393 and 423 K at different ϕ. The values of decreases with increasing ϕ until it attains the minimum value and starts to increase again with ϕ. Due to less quantity of fuel in lean fuel mixtures, the explosion was not brisk, therefore, the combustion time was prolonged. Moreover, reverse reflection is true for increased ϕ. Here values presented in Fig. 14 are in someway sensitive to p_i and T_i. By and large, the values of somehow increased with increased p_i and decreased with increased T_i. An increment in T_i caused a decrease in owing to a faster flame speed. However, at rich mixtures the influence of T_i on the explosion time is somewhat insignificant. This could be as a consequence of equivalence ratio effects on the explosion pressure rise in rich mixtures. Fig. 15 also shows the relationship between p_i and at ϕ = 0.8, 1.0, and 1.2 and T_i = 423 K. According to Fig. 15, somewhat p_i exhibits a close linear correlation with at the different equivalence ratios. Explosion time is closely associated with the flame speed, so, the fastness of the flame speed determines the explosion time. In this study, the explosion time was relatively longer when p_i increased. Thus, when p_i was increased the mass or density of MF mixture also increased which extended the explosion time due to low flame speed. A parallel remark was made in these treatises (Cui et al., 2018; Hu et al., 2017; Xu et al., 2019).

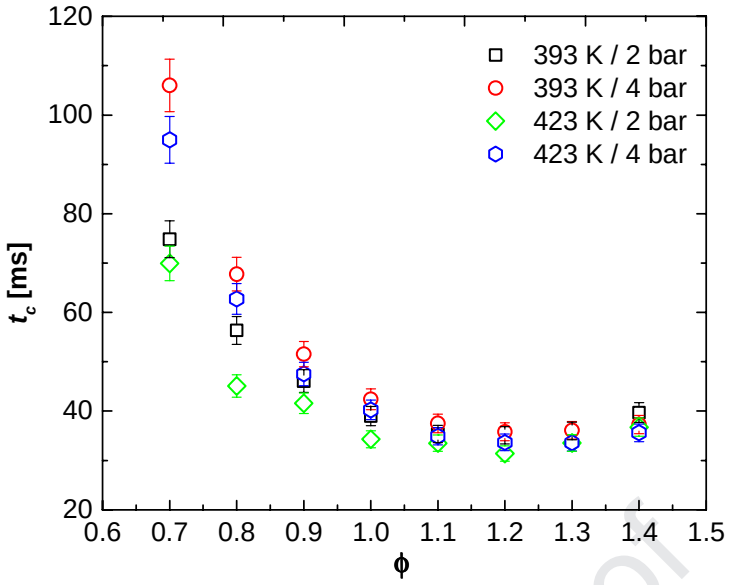

Fig. 14. A plot of with ϕ at p_i = 2 and 4 bar and T_i = 393 and 423 K. Legend: p_i is led by T_i.

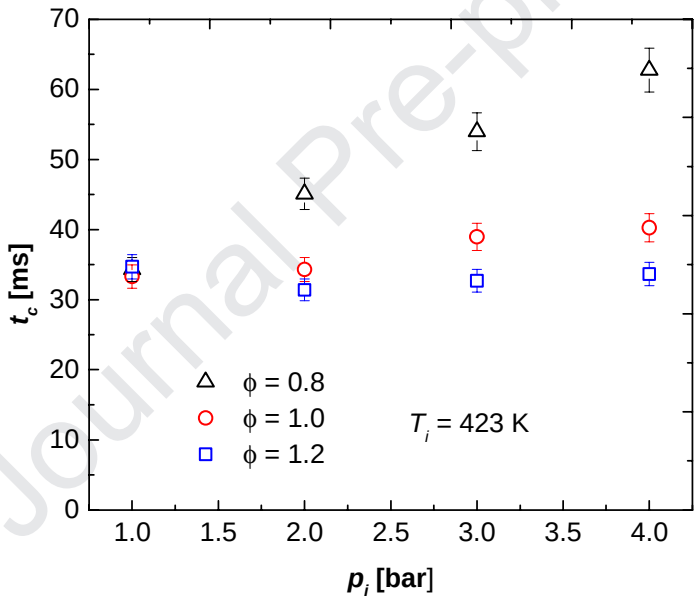

Fig. 15. A graph of against p_i at ϕ = 0.8,1.0, and 1.2 and T_i = 423 K.

3.4. 2-methylfuran LBV

Using the well-established burning velocity relation in equation (1), the pressure history data were used to determine the experimental burning velocities of MF at the investigated conditions. The LBVs at the initial conditions were evaluated from the $S_L(p)$ curve employing extrapolation (Dahoe and de Goey, 2003; Omari and Tartakovsky, 2016; Shen et al., 2017a).

$$S_L = \frac{1}{(p_{\max}-p_i)}\frac{1}{3}\left(\frac{4\pi}{3V}\right)^{-1/3}\left(\frac{p_i}{p}\right)^{1/\gamma}\left[1-\left(\frac{p_i}{p}\right)^{1/\gamma}\left(\frac{p_{\max}-p}{p_{\max}-p_i}\right)\right]^{-2/3}\frac{dp}{dt} \quad (1)$$

p_{max} and p denote the peak explosion pressure and explosion pressure whereas p_i and γ refer to the initial pressure and the specific heat of the unburnt mixture. V and dp/d refer to the CVCC inner volume and the explosion pressure rise rate. Fig. 16(a)-(b) compares the experimental and simulated burning velocities of MF at p_i = 1 bar and 2 bar as well as T_i = 393 K and 423 K. The simulated LBVs were computed with CANTERA thermochemical code (Goodwin et al., 2017) using Cheng et al. (2017) MF mechanism. It is worth noting that the LBV data of this work at T_i = 363 K have been compared to literature data (Ma et al., 2013a) in (Zhongyang et al., 2018) to validate the accuracy of this investigation. In conformity with Fig. 16(a)-(b), the experimental and the simulated LBVs have a parallel tendency. However, the experimental burning velocities are somehow underpredicted compared to the calculated results.

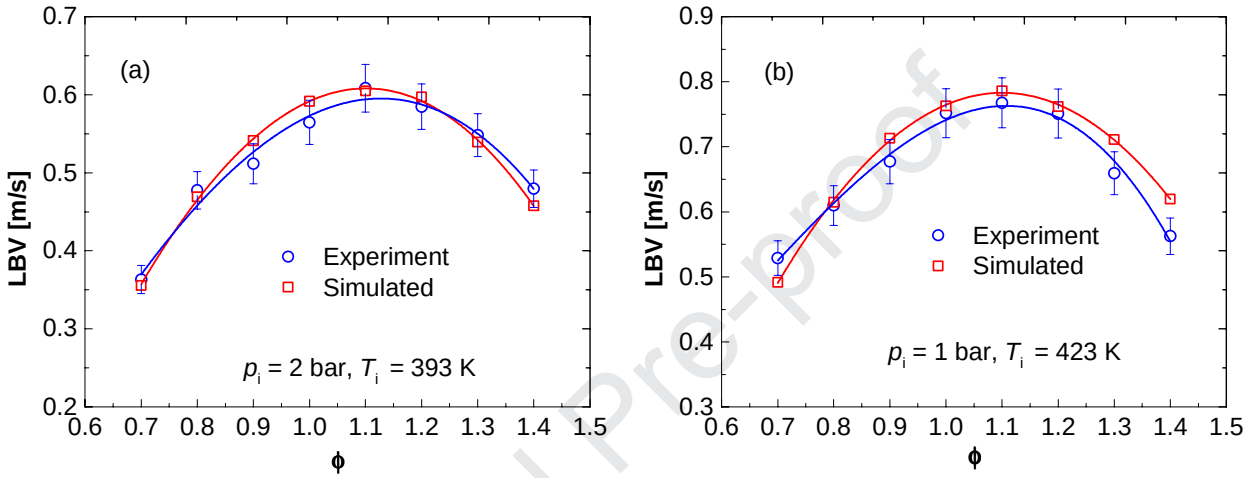

Fig. 16. Comparison of MF experimental and simulated burning velocities. The solid lines represent a polynomial fit.

4. Conclusions

The explosion characteristics of 2-methylfuran have been evaluated at high pressure (1, 2, 3, and 4 bar) and temperature (333-423 K) conditions and equivalence ratio (ϕ = 0.7-1.4) in a constant volume combustion chamber. The important explosion parameters were determined from well-processed pressure data obtained from the experiment. The experimental peak explosion pressure data were compared to simulated data. It was found that the simulated results were higher than the experimental data due to heat loss to the chamber walls during the combustion process in the experiment. The explosion parameters were sensitive to the initial pressure, initial temperature and equivalence ratio. 2-methylfuran peak explosion pressure, maximum pressure rise rate and the deflagration index decreased with increased initial temperature, however, they increased with increased initial pressure. In addition, the magnitude of the explosion parameters increased as the equivalence ratio increased. The deflagration index of 2-methylfuran was found to be quite higher at higher pressures, reactive, and rich mixtures. In conclusion, the explosion time somehow decreased with increased initial temperature and increased with a higher initial pressure.

Acknowledgements

The authors are grateful to the National Key R&D Program of China (No. 2018YFB1501405), the National Natural Science Foundation of China (No. 91741203), and the Hangzhou Science Committee (No.20162013A06) of China for funding this work.

References:

Askari, M.H., Ashjaee, M., Karaminejad, S., 2017. Experimental and numerical investigation of the laminar burning velocity and combustion characteristics of biogas at high pressures. Energy and Fuels 31, 14169–14179.

Bao, X., Jiang, Y., Xu, H., Wang, C., Lattimore, T., Tang, L., 2017. Laminar flame characteristics of cyclopentanone at elevated temperatures. Appl. Energy 195, 671–680.

Beck, M., 2016. The risk implications of globalisation: An exploratory analysis of 105 major industrial incidents (1971-2010). Int. J. Environ. Res. Public Health 13, 1–21.

Cheng, Z., Niu, Q., Wang, Z., Jin, H., Chen, G., Yao, M., Wei, L., 2017. Experimental and kinetic modeling studies of low-pressure premixed laminar 2-methylfuran flames. Proc. Combust. Inst. 1295–1302.

Cui, G., Wang, S., Liu, J., Bi, Z., Li, Z., 2018. Explosion characteristics of a methane/air mixture at low initial temperatures. Fuel 234, 886–893.

Dahoe, A.E., 2005. Laminar burning velocities of hydrogen-air mixtures from closed vessel gas explosions. J. Loss Prev. Process Ind. 18, 152–166.

Dahoe, A.E., de Goey, L.P.H., 2003. On the determination of the laminar burning velocity from closed vessel gas explosions. J. Loss Prev. Process Ind. 16, 457–478.

Di Sarli, V., Benedetto, A. Di, 2012. Sensitivity to the presence of the combustion submodel for large eddy simulation of transient premixed flame-vortex interactions. Ind. Eng. Chem. Res. 51, 7704–7712.

Faghih, M., Gou, X., Chen, Z., 2016. The explosion characteristics of methane, hydrogen and their mixtures: A computational study. J. Loss Prev. Process Ind. 40, 131–138.

Goodwin, D.G., Moffat, H.K., Speth, R.L., 2017. Cantera: An Object-oriented Software Toolkit for Chemical Kinetics, Thermodynamics, and Transport Processes.

Hu, E., Tian, H., Zhang, X., Li, X., Huang, Z., 2017. Explosion characteristics of n-butanol/iso-octane-air mixtures. Fuel 188, 90–97.

Huzayyin, A.S., Moneib, H.A., Shehatta, M.S., Attia, A.M.A., 2008. Laminar burning velocity and explosion index of LPG-air and propane-air mixtures. Fuel 87, 39–57.

Kundu, S.K., Zanganeh, J., Eschebach, D., Badat, Y., Moghtaderi, B., 2018. Confined explosion of methane-air mixtures under turbulence. Fuel 220, 471–480.

Li, D., Zhang, Q., Ma, Q., Shen, S., 2015. Comparison of explosion characteristics between hydrogen/air and methane/air at the stoichiometric concentrations. Int. J. Hydrogen Energy 40, 8761–8768.

Li, Q., Cheng, Y., Huang, Z., 2015. Comparative assessment of the explosion characteristics of alcohol-air mixtures. J. Loss Prev. Process Ind. 37, 91–100.

Li, Y., Bi, M., Huang, L., Liu, Q., Li, B., Ma, D., Gao, W., 2018a. Hydrogen cloud explosion evaluation under inert gas atmosphere. Fuel Process. Technol. 180, 96–104.

Li, Y., Bi, M., Li, B., Zhou, Y., Gao, W., 2018b. Effects of hydrogen and initial pressure on flame

characteristics and explosion pressure of methane/hydrogen fuels. Fuel 233, 269–282.
Ma, X., Jiang, C., Xu, H., Ding, H., Shuai, S., 2013a. Laminar burning characteristics of 2-methylfuran and isooctane blend fuels. Fuel 116, 281–291.
Ma, X., Jiang, C., Xu, H., Shuai, S., Ding, H., 2013b. Laminar burning characteristics of 2-methylfuran compared with 2,5-dimethylfuran and isooctane. Energy and Fuels 27, 6212–6221.
Mannaa, O., Mansour, M.S., Roberts, W.L., Chung, S.H., 2015. Laminar burning velocities at elevated pressures for gasoline and gasoline surrogates associated with RON. Combust. Flame 162, 2311–2321.
Mitu, M., Brandes, E., 2017. Influence of pressure, temperature and vessel volume on explosion characteristics of ethanol/air mixtures in closed spherical vessels. Fuel 203, 460–468.
Mitu, M., Brandes, E., 2015. Explosion parameters of methanol-air mixtures. Fuel 158, 217–223.
Mitu, M., Brandes, E., Hirsch, W., 2018. Mitigation effects on the explosion safety characteristic data of ethanol/air mixtures in closed vessel. Process Saf. Environ. Prot. 117, 190–199.
Mitu, M., Giurcan, V., Razus, D., Oancea, D., 2012. Temperature and pressure influence on ethane-air deflagration parameters in a spherical closed vessel. Energy and Fuels 26, 4840–4848.
Mitu, M., Razus, D., Giurcan, V., Oancea, D., 2015. Normal burning velocity and propagation speed of ethane-air: Pressure and temperature dependence. Fuel 147, 27–34.
OECD, 2013. 25 years of chemical accident prevention at OECD.
Omari, A., Tartakovsky, L., 2016. Measurement of the laminar burning velocity using the confined and unconfined spherical flame methods - A comparative analysis. Combust. Flame 168, 127–137.
Reyes, M., Tinaut, F. V., Horrillo, A., Lafuente, A., 2018. Experimental characterization of burning velocities of premixed methane-air and hydrogen-air mixtures in a constant volume combustion bomb at moderate pressure and temperature. Appl. Therm. Eng. 130, 684–697.
Saeed, K., 2017. Determination of the explosion characteristics of methanol – Air mixture in a constant volume vessel. Fuel 210, 729–737. https://doi.org/10.1016/j.fuel.2017.09.004
Shen, X., Xiu, G., Wu, S., 2017a. Experimental study on the explosion characteristics of methane/air mixtures with hydrogen addition. Appl. Therm. Eng. 120, 741–747.
Shen, X., Zhang, B., Zhang, X., Xiu, G., 2017b. Explosion characteristics of methane-ethane mixtures in air. J. Loss Prev. Process Ind. 45, 102–107.
Somers, K.P., Simmie, J.M., Gillespie, F., Burke, U., Connolly, J., Metcalfe, W.K., Battin-Leclerc, F., Dirrenberger, P., Herbinet, O., Glaude, P.A., Curran, H.J., 2013. A high temperature and atmospheric pressure experimental and detailed chemical kinetic modelling study of 2-methyl furan oxidation. Proc. Combust. Inst. 34, 225–232.
Sun, Z.Y., 2018. Laminar Explosion Properties of Syngas. Combust. Sci. Technol. 1–16.
Sun, Z.Y., Li, G.X., 2017. Turbulence influence on explosion characteristics of stoichiometric and rich hydrogen/air mixtures in a spherical closed vessel. Energy Convers. Manag. 149, 526–535.
Tang, C., Zhang, S., Si, Z., Huang, Z., Zhang, K., Jin, Z., 2014. High methane natural gas/air explosion characteristics in confined vessel. J. Hazard. Mater. 278, 520–528.
Tran, M.V., Scribano, G., Chong, C.T., Ho, T.X., 2017. Influence of hydrocarbon additions and dilutions on explosion behavior of syngas/air mixtures. Int. J. Hydrogen Energy 42, 27416–27427.

World Health Organization, 2009. Manual for the public health management of chemical incidents, World Health Organization.

Wu, Y.-C., Laiwang, B., Shu, C.-M., 2019. Investigation of an explosion at a styrene plant with alkylation reactor feed furnace. Appl. Sci. 9, 503.

Xie, Y., Wang, J., Cai, X., Huang, Z., 2016. Pressure history in the explosion of moist syngas/air mixtures. Fuel 185, 18–25.

Xu, C., Fang, D., Luo, Q., Ma, J., Xie, Y., 2014. A comparative study of laser ignition and spark ignition with gasoline-air mixtures. Opt. Laser Technol. 64, 343–351.

Xu, C., Wang, H., Li, X., Zhou, W., Wang, C., Wang, S., 2019. Explosion characteristics of a pyrolysis biofuel derived from rice husk. J. Hazard. Mater. 369, 324–333.

Xu, C., Zhong, A., Wang, H., Jiang, C., Sahu, A., Zhou, W., Wang, C., 2018. Laminar burning velocity of 2-methylfuran-air mixtures at elevated pressures and temperatures: Experimental and modeling studies. Fuel 231, 215–223.

Zhang, L., Ma, H., Pan, J., Shen, Z., Wang, L., Liu, R., Zhao, K., 2019a. Effects of hydrogen addition on the explosion characteristics of n-hexane/air mixtures. Int. J. Hydrogen Energy 44, 2029–2038.

Zhang, L., Ma, H., Shen, Z., Wang, L., Liu, R., Pan, J., 2019b. Influence of pressure and temperature on explosion characteristics of n-hexane/air mixtures. Exp. Therm. Fluid Sci. 102, 52–60.

Zhongyang, L., Oppong, F., Wang, H., Li, X., Xu, C., Wang, C., 2018. Investigating the laminar burning velocity of 2-methylfuran. Fuel 234, 1469–1480.

Highlights

- Explosion characteristics of 2-methylfuran were studied at elevated pressures and temperatures.
- The influence of initial pressure, initial temperature and equivalence ratio on 2-methylfuran explosion characteristics were assessed.
- The connexion between 2-methylfuran laminar burning velocity and the explosion indices such as the peak explosion pressure, maximum pressure rise rate and the severity factor were examined.